

ARTICLES

Vacuum Thermal Degradation of Poly(ethylene oxide)

Andrei Choukourov,* Andrey Grinevich, Oleksandr Polonskyi, Jan Hanus, Jaroslav Kousal, Danka Slavinska, and Hynek Biederman

Department of Macromolecular Physics, Faculty of Mathematics and Physics, Charles University in Prague, V Holesovickach 2, 18000 Prague 8, Czech Republic

Received: December 5, 2008; Revised Manuscript Received: January 13, 2009

Thermal degradation of poly(ethylene oxide) (PEO) was studied under vacuum conditions. PEO macromolecules degrade predominantly by random chain scission of a backbone with elimination of oligomer fragments. The reactions include the mechanism of radical termination by disproportionation. The eliminated fragments form thin film deposits which have chemical composition close to the original PEO. Activation of the evaporated flux with a glow discharge leads to further fragmentation and recombination of the released species and can be used to tune the properties of the resulting thin films.

Introduction

In the past decades, poly(ethylene oxide) has attracted increasing attention because of its usability in a variety of applications such as drug delivery, gas chromatography, and microbiology, etc. Nonfouling properties of PEO, i.e., its ability to resist accumulation of proteins and cells from biological fluids, are of particular importance.¹ When applied as thin film on a medical instrument or an implant, PEO may significantly or totally prevent unwanted biological adhesion and therefore reduce the risk of bacterial infections.^{1,2} The drawback of PEO film physically adsorbed on the surface is that it leaches, since it is soluble in water. To retain the nonfouling properties over an extended period of time, covalent bonding of PEO chains is required. It has been shown that self-assembled monolayers (SAMs) of PEOs fixed on gold or silicon dioxide surface exhibit stable low bioadhesion.^{1–3} The SAM chemistry however drastically narrows the choice of the substrate material and involves multistep wet treatment. Recently, plasma polymerization methods have been proposed to deposit thin PEO-like films.^{4–7} In these methods, a low-pressure glow discharge is ignited in an atmosphere of organic precursor bearing ether groups. Molecular fragmentation with the formation of free radicals is initiated by an electron impact, and radical polymerization proceeds on adjacent surfaces. The resultant films of plasma polymers have a network structure with composition depending on the parameters of the deposition. The low discharge power and modulated regime produce films with a high retention of PEO structure.

This work offers vacuum thermal degradation of PEO as another route for depositing PEO-like thin films without implementation of conventional “wet” chemistry methods. The study of thermal decomposition of polymers was started in 1960s and has been recently renewed when polyimide was subjected to elevated temperature under vacuum.⁸ It has been shown that thermal destruction of polymeric chains proceeds with emission

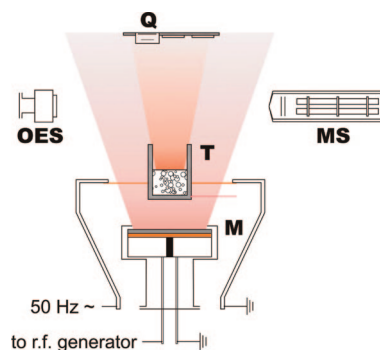


Figure 1. Experimental arrangement: Q, quartz crystal microbalance; OES, optical emission spectroscopy; MS, mass spectrometry; C, crucible; T, thermocouple; M, magnetron.

of low molecular weight fragments which deposit on adjacent surfaces to form a film with a composition very close to the original polymer. When a glow discharge was applied to activate the flux of the released fragments, films with different extents of cross-linking and retention of polyimide structure were obtained. The same strategy is employed here with the aim to present a potential method for depositing PEO-like thin films. The work is divided into two parts. This paper is focused on the diagnostics of the thermal degradation process, whereas a sequel manuscript will deal with detailed characterization of resultant films.

Experimental Methods

Except for the design of the heater, the experimental arrangement was analogous to the one previously used in the experiments with polyimide.⁸ PEO granules (Sigma, $M = 1500$) were loaded into a copper crucible, which rested on two molybdenum stripes heated by electric current (Figure 1). A thermocouple was attached to the crucible to control the temperature of PEO. The crucible was placed 4 cm above a magnetron with a graphite target. The magnetron was used to ignite a glow discharge when required, while graphite was

* To whom correspondence should be addressed. Phone: +420-221912338. Fax: +420-221912350. E-mail: choukourov@kmf.troja.mff.cuni.cz.

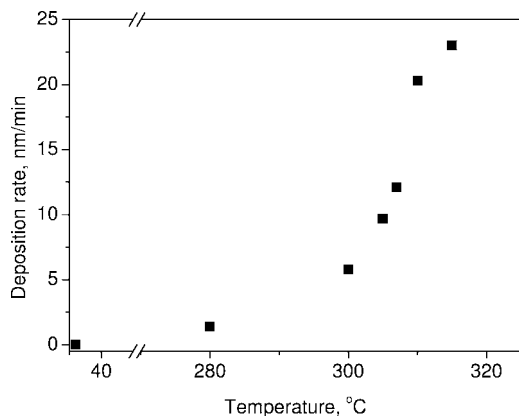


Figure 2. Deposition rate of PEO-like film.

chosen as a material with low-sputter yield to minimize the contribution of sputtered carbon to deposited films. A radio frequency (rf) generator (Dressler Ceasar 13.56 MHz) was used to deliver power to the magnetron. A quartz crystal microbalance (QCM) was placed in the plane with the substrates 10 cm above the crucible. The entire arrangement resided in a vacuum chamber brought by rotary and diffusion pumps to a base pressure of 1×10^{-3} Pa. The experiments were performed with and without argon used as a gas to initiate the plasma. In the case of depositions with argon, 1 Pa pressure and $5 \text{ cm}^3(\text{STP}) \text{ min}^{-1}$ flow rate were used.

The heating process was monitored by a mass spectrometer (Hiden Analytical, HAL 301 RC, 70 eV electron energy) as well as by an optical emission spectrometer (Action Research SpectraPro 300i) when plasma was applied.

The reference mass spectra of diethylene glycol (DEG, Sigma, $M = 106$) and triethylene glycol (TEG, Sigma, $M = 150$) were also measured. For this purpose, a liquid monomer was poured into the crucible and the chamber was evacuated to the monomer vapor pressure. The mass spectrum of DEG was acquired at ~ 0.1 Pa and at room temperature, while in the case of TEG the vapor pressure was too low and the monomer was heated to 40°C to increase its pressure to ~ 0.1 Pa.

Fourier transform infrared reflection absorption spectroscopy (FTIR-RAS, Bruker Equinox 55) and X-ray photoelectron spectroscopy (XPS, Phobios 100, Specs) were utilized to analyze the chemical composition of the deposits. Furthermore, a chemical derivatization technique was used to determine the concentration of OH groups as described elsewhere.⁹ Briefly, the film deposited on the glass substrate was brought in contact with vapors of trifluoroacetic anhydride (TFAA), which selectively tags the hydroxyl groups. After completion of the reaction, the surface elemental composition including fluorine was determined by XPS and the concentration of hydroxyl groups was calculated (for details see the Supporting Information).

Results and Discussion

After adjusting the pressure and flow rate of argon, the heater current was set at a constant value of 40 A, and the heating process was started. Simultaneously, the mass spectra and the values of the crucible temperature were recorded. PEO started to melt at about 60°C ; the melting was visualized through a chamber window. However, it was not until 260°C when QCM detected first deposition and the mass spectra revealed changes in the gaseous phase composition. Figure 2 shows the deposition rate recalculated from the values of QCM frequency shift as a function of temperature. In preliminary experiments, the crucible

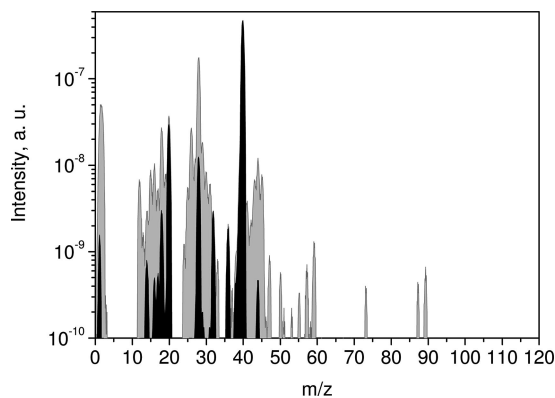


Figure 3. Mass spectra of the gaseous phase in the reactor volume (Ar, 1 Pa): black, PEO at 25°C ; gray, PEO at 320°C .

temperature was stabilized at a certain value which was checked both by a thermocouple and by the QCM frequency shift being constant with time. Then a silicon sample with a mask was introduced to the chamber by a load-lock, and the film was allowed to deposit on the sample for 20 min. Afterward, the sample was withdrawn from the deposition zone, the mask removed, the thickness of the film measured by AFM, and the deposition rate calculated. Finally, a calibration factor of QCM was estimated in terms of hertz per nanometer; this was then used to calculate the deposition rate in the mass spectral experiments. Obviously, the dependence of the deposition rate on temperature is not linear. The deposition rate increases almost exponentially and reaches 25 nm/min at 320°C . In contrast to the experiments with polyimide,⁸ where carbonaceous residue was found in the heater after the deposition, here the entire PEO load disappeared after extended heating.

Figure 3 shows the mass spectra taken under 1 Pa argon pressure at room temperature and at 320°C . The spectrum acquired at room temperature (black color) consists of the species with $m/z < 45$. As expected, the most abundant species is argon (Ar^+ and Ar^{2+} with $m/z = 40$ and 20). Residual air is detected through the $m/z = 14$ and 28 (N_2), 16 and 32 (O_2), 18 (H_2O), and 44 (CO_2).

The mass spectrum acquired at 320°C (gray color) reveals significant changes as compared to 25°C . Since the pressure of argon was held constant, the intensity of the lines with $m/z = 20$ and 40 did not change over the entire experiment. The leak into the chamber from the outer atmosphere was checked to be constant before and after the deposition; therefore, all the changes detected in the mass spectra can be attributed to emission of the volatile fragments from the PEO melt. The most drastic changes are observed for $m/z = 1-2$, $12-18$, $24-34$, 44 , and above. An almost 2 orders of magnitude increase of the hydrogen signal is explained by the cleavage of the CH and OH bonds of PEO molecules. The $m/z = 12-18$ assigned to C, CH_x , OH, and H_2O are also enhanced but not as much as hydrogen. The strong increase of the $m/z = 28$ can be assigned to emission of C_2H_4 and CO. The $m/z = 44$ and around are attributed to a number of the fragments of the PEO backbone such as $\text{CH}_2\text{CH}_2\text{O}$, CH_3COH , $\text{CH}_3\text{-O-CH}_3$, and $\text{CH}_3\text{-CH}_2\text{-OH}$ or to CO_2 . The spectrum at 320°C is also characterized by the presence of higher m/z , which belong to the fragments with more than one monomer unit.

Since the mass spectra were acquired continuously with heating, it was possible to monitor the evolution of the individual peaks. Figure 4 shows the dependence of hydrogen, $\text{CO}/\text{C}_2\text{H}_4$, and H_2O on the temperature of the PEO melt; other species are not shown for simplicity. All intensities were normalized to Ar,

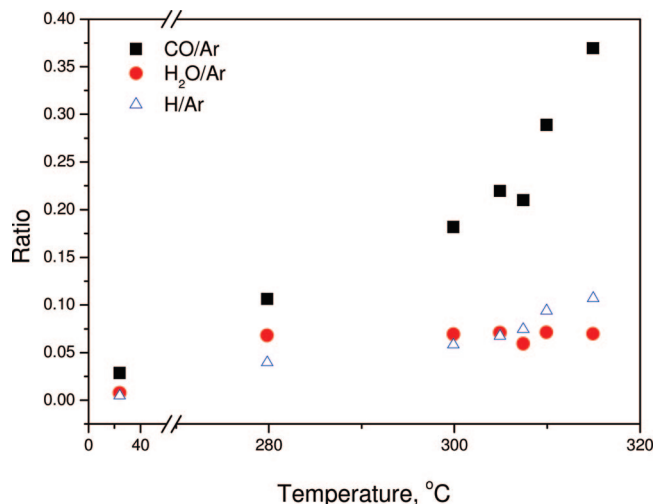


Figure 4. Evolution of the mass spectrum with temperature of PEO.

$m/z = 40$. Starting from 260 °C, most of the mass spectral bands show an increase with respect to argon except for H_2O , which stays at a constant level throughout the entire temperature range. The strongest increase is apparent for the $\text{CO}/\text{C}_2\text{H}_4$ peak. Thus, thermal degradation of PEO proceeds with the scission of the polymeric chains and elimination of volatile species with a wide distribution of molecular weights.

The next experiment was performed without argon in the chamber. After evacuating the system to 10^{-3} Pa the heating was started. When the temperature reached 320 °C, the valve between the chamber and the diffusion pump was throttled to set the pressure at 1 Pa. The gaseous medium in the chamber was composed in this case of the emitted fragments of PEO and of residual gases. The mass spectrum taken under such conditions reflects the increased partial pressure of the volatile PEO fragments (Figure 5a). The spectrum of residual gases at 25 °C is also shown here for reference.

A wide spectrum of the species is observed in Figure 5a, with the highest m/z detected at 112. One should bear in mind that PEO undergoes two stages of fragmentation: the first is decomposition in the crucible by the influence of elevated temperature and the second is fragmentation of evaporated species of unknown composition in the ionization source of the mass spectrometer. Consequently, the fragmentation pattern measured by the detector in the mass spectrometer is very diverse, giving rise to uncertainty about the origin of the ions. The conventional way to come around this problem and identify the unknown compound is to compare its spectrum with those of compounds of defined composition. Certain guesses should be made beforehand to choose the appropriate reference. In our case, it can be noticed that starting from $m/z = 44$ the spectrum consists of a series of lines similar in shape and with the maxima separated by $\Delta m/z = 14$ or 16, which is reasonable to assign to the $-\text{CH}_2-$ and $-\text{O}-$ residues of the polymeric backbone (see also Table 1). Such assumption is also supported by comparison of the bond energies. The dissociation energy of the $\text{C}-\text{O}-\text{C}$ and $\text{C}-\text{C}-\text{O}$ bond is lower compared to $\text{C}-\text{H}$,¹⁰ and hence it is generally expected that decomposition of PEO starts with the random scission of the backbone bonds. On the assumption that the volatile fragments are composed of the combination of $-\text{CH}_2-$ and $-\text{O}-$ groups, their molecular structure can be guessed by comparison against the mass spectra of ethylene glycol homologues of known composition. Parts b and c of Figure 5 show the spectra of di- and triethylene glycol ($M = 106$ and 150,

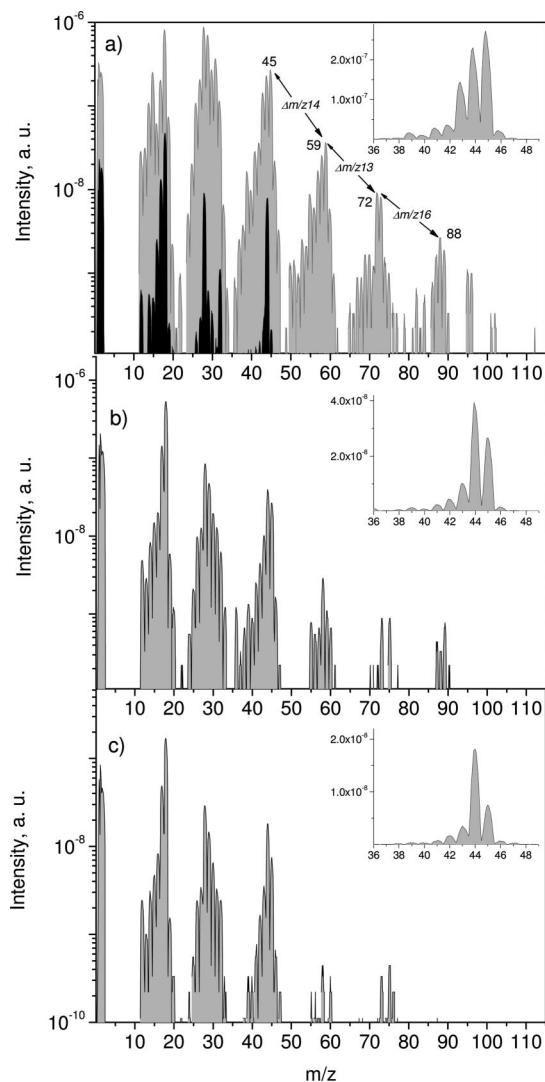


Figure 5. Mass spectra of the gaseous phase in the reactor volume without Ar: (a) PEO at 25 °C (black) and at 320 °C (gray); (b) TEG at 40 °C; (c) DEG at 25 °C.

TABLE 1: Assignment of the Most Intensive Mass Spectral Lines

species	calculated m/z	detected maxima
$-\text{CH}_2-\text{CH}_2-\text{O}-$	44	45
$-\text{CH}_2-\text{CH}_2-\text{O}-\text{CH}_2-$	58	59
$-\text{CH}_2-\text{CH}_2-\text{O}-\text{CH}_2-\text{CH}_2-$	72	73
$-\text{CH}_2-\text{CH}_2-\text{O}-\text{CH}_2-\text{CH}_2-\text{O}-$	88	88
$-\text{CH}_2-\text{CH}_2-\text{O}-\text{CH}_2-\text{CH}_2-\text{O}-\text{CH}_2-$	102	103

respectively), the spectra of other homologues not shown because of their close similarity. The molecular ion peak, i.e., the monomer molecule with one electron removed, does not appear at all in the two cases. The fragmentation pattern consists of the bands centered at $m/z = 2, 18, 28, 44, 58, 73$ and, in the case of TEG, at $m/z = 89$, which is almost identical to the pattern observed for evaporation of PEO. With increasing mass in the homologous series (di- and triethylene glycol) the spectra remain almost unchanged, implying that the fragmentation phenomena occur in the same manner regardless of the molecular mass of the monomer. The close similarity of the mass spectra of evaporated PEO and ethylene glycols proves that the vapor phase in experiments with poly(ethylene oxide) is mainly composed of PEO oligomers with a different number of monomer units.

The absence of the signal for $m/z > 102$ does not necessarily mean that such fragments are not present in the chamber volume as the mass spectra of ethylene glycols do not show the species of higher m/z either. The long distance between the detector and the evaporation source limits the transport of heavy particles to the ionization chamber. Furthermore, transmission function of the quadrupole is mass-dependent, and its poor sensitivity to ions of higher mass also restricts their detection. Fares et al. have characterized the degradation products of PEO by pyrolysis mass spectrometry.¹¹ The direct pyrolysis technique (with the evaporation source placed within the mass spectrometer) detected fragments of the type $\text{CH}_3\text{CH}_2\text{O}(\text{CH}_2\text{CH}_2\text{O})_n\text{CH}_2$, where n reached 6. However, indirect analysis with the evaporation source placed in a remote chamber observed no species above $m/z = 100$.

Regardless of the close similarity between the mass spectra of di-/triethylene glycols and evaporated PEO several different features can also be noticed. First, the presence of the low mass species in the spectra of di- and triethylene glycol indicates that the fragmentation of the monomers occurs in the ionization source of the spectrometer, and therefore the mass spectrum of evaporated PEO, which is also rich in light masses, hardly represents accurately the actual fragmentation induced purely by thermal means. It can be noted, however, that unlike ethylene glycols, in the case of PEO the $m/z = 28$ is the strongest which means that CO, and probably C_2H_4 , is released not only as a result of fragmentation phenomena in the mass spectrometer but also due to thermal degradation of the original polymer. Further discrepancy between ethylene glycol homologues and PEO can be observed at higher m/z in intensity of the species with $M - n$ ($n = 1, 2, 3, \dots$), where M is m/z of the most intensive peak of the individual bands. In the case of ethylene glycols, abundance of the species with $M - n$ is much smaller than that of the base peak (see also the insets of Figure 5a–c). In contrast, wider distribution of m/z is detected for evaporated PEO and their intensity is stronger. This indicates that such species may not be formed exclusively in the ionization chamber of the mass spectrometer but are rather emitted into the chamber volume in the evaporation process. The presence of the species with m/z several units less than a simple sum of CH_2 and O implies that these fragments are strongly dehydrogenated; this is further supported by the strong signal from hydrogen $m/z = 1$ –2. Cleavage of a hydrogen atom leaves a free radical or, if two hydrogen atoms are removed from the neighboring carbons, the recombination of the radicals with formation of the double $\text{C}=\text{C}$ bond is possible. Nevertheless, such dehydrogenated species are in minority with respect to PEO oligomers—see, for example, the rapidly decreasing intensity of the left-hand side shoulder of the band centered at $m/z = 59$ in Figure 5. Interestingly, the maxima of the bands of evaporated PEO are located at the m/z which exceed by 1 those calculated for a combination of the CH_2 and O species. This means that capture of hydrogen atoms by oligomeric fragments also takes place. The contribution from higher isotopes (^2H , ^{13}C , or ^{17}O) can be ruled out here as their natural abundance in the corresponding elements is low.¹⁰ Taking into account the appearance of both the dehydrogenated species and the species with excess of hydrogen, the possible mechanism of PEO decomposition is radical termination by disproportionation, when a radical at the end of one chain attacks hydrogen atom in the other chain.¹² As a result, a hydrogen atom is transferred to the first chain and a double bond is created in the other as shown in an example below (Figure 6). Depending on the species, the hydrogen transfer may proceed

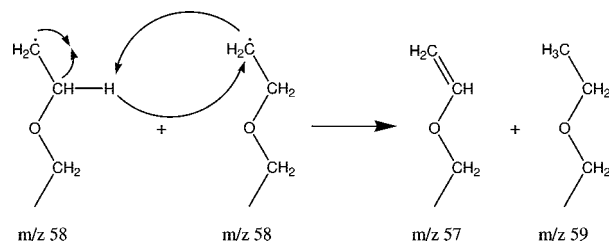


Figure 6. Radical termination by disproportionation.

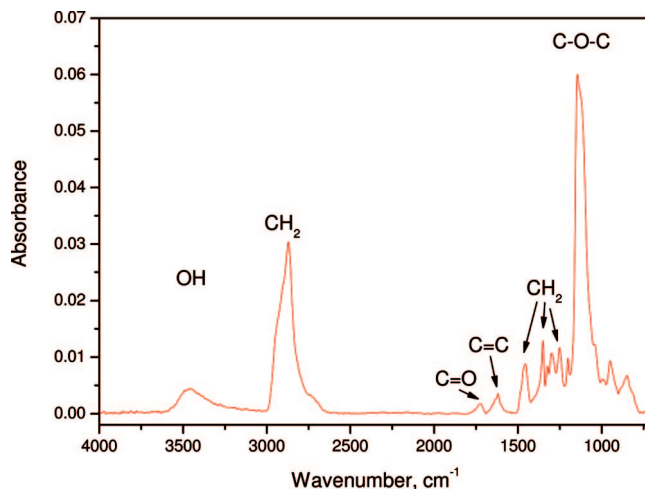


Figure 7. FTIR spectrum of the film deposited by vacuum thermal degradation of PEO.

on the $-\text{CH}_2$ and/or on the $-\text{O}$ termini of the oligomeric species, yielding $-\text{CH}_3$ and $-\text{OH}$ chain ends.

The formation of the $\text{C}=\text{C}$ functional groups was further confirmed by FTIR spectroscopy of the deposited film. A broad band at $\sim 3450\text{ cm}^{-1}$ in Figure 7 belongs to the OH groups, but formation of hydroxyls during thermal fragmentation of PEO cannot be argued here as they are present as the end groups in the original polymer. A band centered at 2870 cm^{-1} is assigned to symmetric stretching vibrations of the CH_x groups. Corresponding asymmetric stretching vibrations of the CH_x groups are seen as the left-hand side shoulder at 2935 cm^{-1} . The subscript x indicates here that hydrocarbons with different amount of hydrogen may be responsible for absorption in this region. However, the shape of this peak is very similar to that of the original PEO (see the Supporting Information), and it can be therefore suggested that CH and CH_3 groups are in the minority and their absorption is subdued by the CH_2 functionalities.

The $\text{C}=\text{C}$ bonds are detected at 1620 cm^{-1} . Note also the weak band at 1730 cm^{-1} , which can be unambiguously assigned to the $\text{C}=\text{O}$ -based species. The most intensive peak is located at 1100 cm^{-1} and attributed to the $\text{C}-\text{O}-\text{C}$ functional group. The spectrum is also characterized by various deformation vibrations of CH_2 groups in the 1200 – 1450 cm^{-1} region.

Undetectable absorption of CH_3 groups relative to CH_2 and the strong signal from $\text{C}-\text{O}-\text{C}$ indicate a good retention of PEO structure in the deposited film. The relative concentrations of $\text{C}=\text{C}$, $\text{C}=\text{O}$, and $\text{C}-\text{O}-\text{C}$ groups can hardly be estimated from the FTIR spectra as dipole moments of these functionalities are very different. The XPS C 1s spectrum in Figure 8 supplements the FTIR analysis and shows significant retention of ether structure. Almost 80% of carbon atoms are bound in $\text{C}-\text{O}-\text{C}$ species (the peak at 286.5 eV), while carbonyls (287.8 eV) and aliphatic hydrocarbons (285.0 eV) are in the minority.

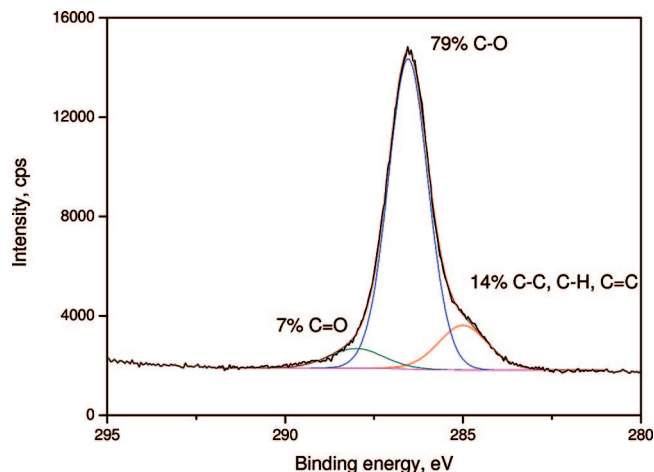


Figure 8. XPS C 1s peak of the film deposited by vacuum thermal degradation of PEO.

The peak at 286.5 eV assigned here to ethers can generally be contributed to by epoxy and hydroxy groups. Characteristic absorption of epoxides at 1270 cm^{-1} was not observed in the FTIR spectrum, and they can therefore be excluded from the consideration. The chemical derivatization test with TFAA was performed to estimate the concentration of hydroxyls. The results showed that only up to 2% of carbon atoms are bound to OH groups so that the assignment of the second component in the XPS C1s peak to C—O—C functionality is justified. It is also worth noting that XPS of original PEO gives 88% of the C—O—C groups (see the Supporting Information), and hence the chemical composition of the resultant film is very close to that of conventional polymer.

The films deposited by pyrolysis of conventional polymers were frequently reported in the literature as being “waxlike” since such films are mainly composed of the lower molecular weight fragments of original macromolecules.^{13,14} Different postdeposition treatment methods were suggested to increase the cross-linking within the films, including UV irradiation and annealing.¹⁵ Ionization-assisted evaporation was also considered to ionize the volatile fragments by electron impact and direct them onto negatively biased substrate.^{16,17} Here, the stream of evaporated species was allowed to pass through a glow discharge zone. Glow discharge sustained in organic vapors is known to produce a vast number of active species and UV irradiation, which can induce and promote different polymerization pathways. Figure 9 shows the mass spectra of the chosen species measured without the discharge and with 5 and 60 W plasma turned on. Obviously, the application of the glow discharge leads to a drastic increase of atomic and molecular hydrogen concentration as a result of ablation of hydrogen from the macromolecular fragments by electron impact. Another species showing an increase in concentration upon turning on the plasma is $m/z = 28$, though in this case such an increase is not so significant. The CO molecules are the most possible species responsible for this peak as their presence was confirmed by the independent OES measurements which will be discussed below. The reverse behavior is seen for the higher masses where even 5 W plasma results in a decrease of their amount. No species above $m/z = 60$ were detected with active plasma. The disappearance of the signal from the higher masses upon switching on the discharge is attributed partly to the enhanced fragmentation of the volatile species. However, the dissociation rates under these conditions are unlikely to reach high values, and this effect is related to a larger extent to the heterogeneous

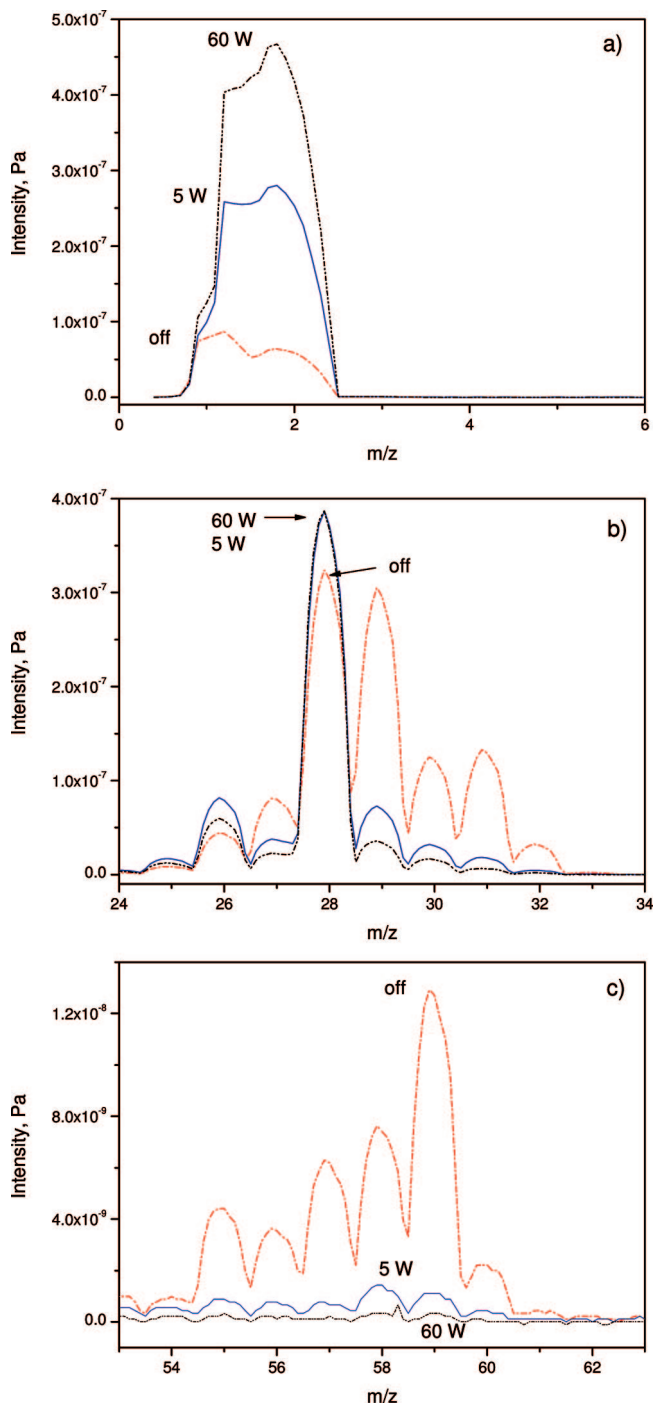


Figure 9. Mass spectra of PEO evaporated with and without plasma: (a) $m/z = 2$; (b) $m/z = 28$; (c) $m/z = 59$.

loss of activated fragments in various recombination reactions during their transport to the detector of the mass spectrometer.

The OES spectra were acquired in two regimes: with argon as a working gas (Figure 10a) and without argon when the discharge was maintained only in the vapors of the volatile products of PEO decomposition (Figure 10b). A complete deciphering of the OES spectra is complicated because of a large number of the species available; however, several bands can be definitely assigned.¹⁸ For example, the fourth positive ($A^1\Pi^+ - X^1\Sigma$) and the 3^d positive ($b^3\Sigma - a^3\Pi$) systems of CO, with the probable contribution of the Cameron and 5B bands were identified. Emission of the OH groups (the $A^2\Sigma^+ - X^2\Pi$ system) was also detected. In addition, the lines of neutral argon

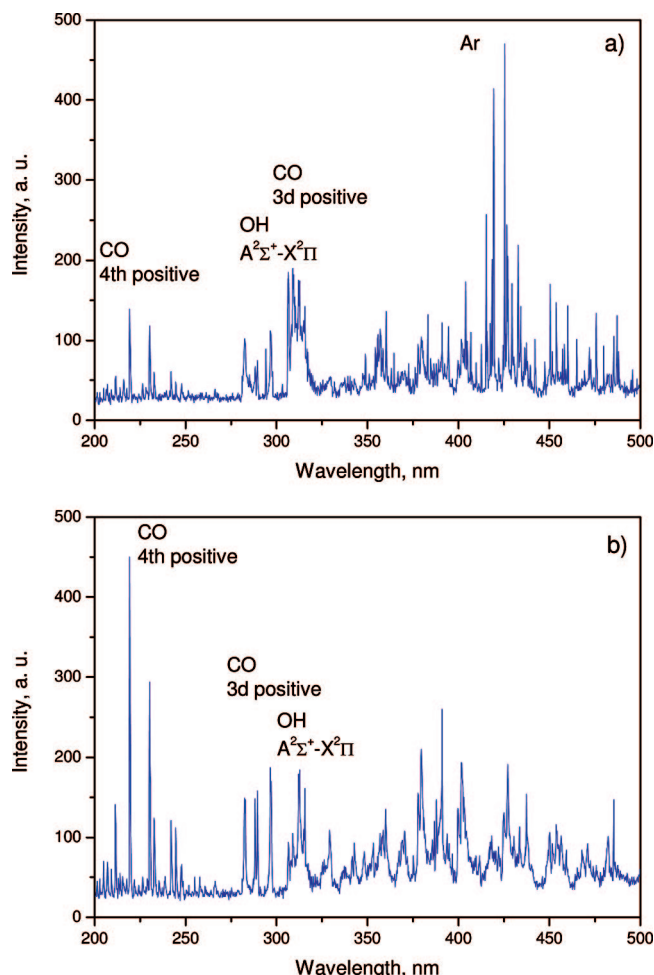


Figure 10. OES of the glow discharge at 50 W power: (a) vapors of PEO with Ar; (b) vapors of PEO without Ar.

were present in the spectrum of the discharge with argon, whereas they vanished when the argon inlet was shut off. Without argon, the emission of CO is significantly enhanced, as can be seen from a comparison of the line of CO at 219.2 nm against the line of OH at 308.8 nm. Note that both spectra were acquired during the same experiment under the same conditions (temperature of PEO, pressure, and power of the discharge) so that the only difference was the composition of the gas phase. The concentration of the OH groups is not much influenced by the action of plasma nor is the concentration of water molecules influenced by the temperature of the PEO melt, as seen in Figure 4. It appears that neither of the fragmentation routes (thermal degradation or fragmentation by electron impact) leads to enhanced release of the OH/H₂O species. This contrasts with thermal degradation of other oxygen-containing polymers such as, for example, poly(vinyl alcohol), which contains hydroxyls as side groups bonded to a hydrocarbon backbone and which degrades with elimination of water.^{11,19–21}

Conclusions

Thermal degradation of PEO proceeds with random scission of the backbone and elimination of volatile species of diverse composition. The low molecular weight fraction is composed of atomic and molecular hydrogen, C, CH_x, OH, H₂O, and CO molecules, hydrogen and CO being the most abundant. The

higher molecular weight fraction consists of fragments of the macromolecular chain differing in the number of (–CH₂–O–) units. Furthermore, oligomers with a lack and with an excess of hydrogen are present in the gas phase, which suggests that radical termination by disproportionation is responsible for this phenomenon. Elimination of water molecules is constant regardless of the temperature of the PEO melt, and therefore it is unlikely to be one of the major routes of PEO thermal degradation. The released oligomeric species form thin film deposits with composition very close to parent PEO. Ether groups constitute about 80% of carbon atoms, whereas hydroxyls are present in such films in an amount of less than 2%. Application of a glow discharge leads to an increase of the low molecular weight fraction of the gas phase due to additional fragmentation of volatile fragments by electron impact. The higher molecular weight species activated by plasma participate in recombination reactions, and enhanced cross-linking of the deposited films is expected. The use of the glow discharge to tune the properties of the films deposited by vacuum thermal degradation of PEO is therefore a promising approach.

Acknowledgment. This work was supported by Grant 202/08/8158 of the Grant Agency of the Czech Republic.

Supporting Information Available: Figures showing FTIR-ATR and the C 1s XPS spectra of conventional PEO used for the vacuum thermal degradation study and text giving details of the chemical derivatization test. This information is available free of charge via the Internet at <http://pubs.acs.org>.

References and Notes

- (1) Kitching, K. J.; Pan, V.; Ratner, B. D. *Biomedical Applications of Plasma-Deposited Thin Films*. In *Plasma Polymer Films*; Biederman, H., Ed.; Imperial College Press: London, 2004; p 392.
- (2) Li, L.; Chen, S.; Zheng, J.; Ratner, B. D.; Jiang, S. *J. Phys. Chem. B* **2005**, *109*, 2934–2941.
- (3) Kingshott, P.; Griesser, H. J. *Curr. Opin. Solid State Mater. Sci.* **1999**, *4*, 403–412.
- (4) Chu, L.-Q.; Knoll, W.; Foersch, R. *Chem. Mater.* **2006**, *18*, 4840–4844.
- (5) Sardella, E.; Gristina, R.; Senesi, G. S.; d'Agostino, R.; Favia, P. *Plasma Process. Polym.* **2004**, *1*, 63–72.
- (6) Johnston, E. E.; Bryers, J. D.; Ratner, B. D. *Langmuir* **2005**, *21*, 870–881.
- (7) Beyer, D.; Knoll, W.; Ringsdorf, H.; Wang, J.-H.; Timmons, R. B.; Sluka, P. *J. Biomed. Mater. Res.* **1997**, *36*, 181–189.
- (8) Choukurov, A.; Hanus, J.; Kousal, J.; Grinevich, A.; Pihosh, Y.; Slavinska, D.; Biederman, H. *Vacuum* **2006**, *80*, 923–929.
- (9) Rinsch, C. L.; Chen, X.; Panchalingam, V.; Eberhart, R. C.; Wang, J.-H.; Timmons, R. B. *Langmuir* **1996**, *12*, 2995–3002.
- (10) Lide, D. R. *Handbook of Chemistry and Physics*, 76th ed.; CRC Press: New York, 1995.
- (11) Fares, M. M.; Hacaloglu, J.; Suzer, S. *Eur. Polym. J.* **1994**, *30* (7), 845–850.
- (12) Hollaender, A.; Thome, J. *Degradation and Stability of Plasma Polymers*. In *Plasma Polymer Films*; Biederman, H., Ed.; Imperial College Press: London, 2004; p 392.
- (13) Luff, P. P.; White, M. *Thin Solid Films* **1970**, *6*, 175–195.
- (14) White, M. *Thin Solid Films* **1973**, *18*, 157–172.
- (15) Boonthanom, N.; White, M. *Thin Solid Films* **1974**, *24*, 295–306.
- (16) Usui, H.; Koshikawa, H.; Tanaka, K. *J. Vac. Sci. Technol. A* **1995**, *13* (5), 2318–2324.
- (17) Usui, H.; Kikuchi, H.; Tanaka, K.; Miyata, S.; Watanabe, T. *J. Vac. Sci. Technol. A* **1998**, *16* (1), 108–113.
- (18) Pearse, R. W. B.; Gaydon, A. G. *The Identification of Molecular Spectra*; Wiley: New York, 1976.
- (19) Ettre, K.; Varadi, P. F. *Anal. Chem.* **1962**, *34* (7), 752–757.
- (20) Smirnov, L. V.; Kulikova, N. P.; Platonova, N. V. *Polym. Sci. U.S.S.R.* **1967**, *9* (11), 2849–2856.
- (21) Peng, Z.; Kong, L.-X. *Polym. Degrad. Stab.* **2007**, *92*, 1061–1071.